

SUPERNOVAE EXPLOSIONS INDUCED BY PAIR PRODUCTION
INSTABILITY

Thesis by

Gary Scott Fraley

In Partial Fulfillment of the Requirements

For the Degree of
Doctor of Philosophy

California Institute of Technology
Pasadena, California

1967

(Submitted April 11, 1967)

ABSTRACT

Stars with a core mass greater than about $30 M_{\odot}$ become dynamically unstable due to electron-positron pair production when their central temperature reaches $1.5-2.0 \times 10^9$ K. The collapse and subsequent explosion of stars with core masses of 45, 52, and $60 M_{\odot}$ is calculated. The range of the final velocity of expansion (3,400-8,500 km/sec) and of the mass ejected ($1-40 M_{\odot}$) is comparable to that observed for type II supernovae.

An implicit scheme of hydrodynamic difference equations (stable for large time steps) used for the calculation of the evolution is described.

For fast evolution the turbulence caused by convective instability does not produce the zero entropy gradient and perfect mixing found for slower evolution. A dynamical model of the convection is derived from the equations of motion and then incorporated into the difference equations.

ACKNOWLEDGEMENTS

The author would like to express his thanks to Dr. R.F. Christy for his advice and suggestions. He would also like to thank the National Aeronautics and Space Administration for financial support.

TABLE OF CONTENTS

PART	TITLE	PAGE
I.	INTRODUCTION.....	1
II.	DIFFERENCE EQUATIONS.....	8
III.	CONVECTION.....	19
IV.	EQUATION OF STATE AND RATES OF ENERGY GENERATION.....	35
V.	EXPLOSIONS OF 45, 52, AND 60 M_{\odot} STARS.....	40
	REMARKS.....	67
	REFERENCES.....	69
	FIGURES.....	71

Chapter 1

INTRODUCTION

In attempts to explain the phenomena of supernovae a number of mechanisms have been proposed as the triggering device of a stellar explosion. Fowler and Hoyle (1960) suggested thermal instability in degenerate stars as the cause of type I supernovae. Thermal instability may be explained briefly as follows. If heat is added to the core of a star it will expand. Thermal instability arises in the case in which the temperature in the core increases; if the instability persists, the temperature increase may raise the rate of energy generation until the evolution reaches an explosive time scale. If we assume that the envelope responds by expanding uniformly, to maintain hydrostatic equilibrium the pressure in the core must change proportionally to the $4/3$ power of the density. Whether or not the temperature rises in the core depends on whether or not the (appropriately averaged) value of $(\partial \log P / \partial \log \rho)_T$ in the core is greater or less than $4/3$.

If the value of $\gamma (= (\partial \log P / \partial \log \rho)_s)$ of the envelope (which expands isentropically) is $4/3$, the envelope will respond to any change in the core by expanding uniformly, and the assumption is satisfied. When γ is greater than $4/3$, the pressure in the uniform expansion

drops too rapidly to maintain hydrostatic equilibrium. The degree of expansion must decline toward the surface; since the mass of the envelope is closer to the center, the value of $(d \log P / d \log \rho)$ in the core must now be somewhat less than $4/3$. This value is the critical value of $(\partial \log P / \partial \log \rho)_T$ for thermal instability. The instability depends not only on the stellar structure, but on the way in which the heat absorption is distributed, as the core referred to is the region in which the energy is effectively absorbed. The instability requires a higher degree of degeneracy for relativistic material (for which $(\partial \log P / \partial \log \rho)_T = 4/3$ for total degeneracy) than for non-relativistic material (for which it is $5/3$). Characteristically the degree of degeneracy is greater for points closer to the center. The central temperature may therefore increase when the star contracts due to neutrino losses (which are spread over a large part of the star), and then continue to increase as the star begins to expand when nuclear energy generation (which is concentrated near the center) becomes greater than the neutrino losses.

Fowler and Hoyle proposed that the instability would cause explosions in stars with masses slightly above the Chandrasekhar limit, which would be relativistically degenerate at temperatures high enough to burn oxygen or silicon. Investigations of the instability were carried out by the author for oxygen and silicon burning. If convection is

neglected all the heat is deposited in a small highly degenerate core, and the evolution does reach an explosive time scale. The effect of the convection spreads the energy generated over a larger less degenerate region, and the instability disappears long before the nuclear burning reaches an explosive rate. Shaviv (1966), who followed the advanced evolution of stars above the Chandrasekhar limit, also found no explosions due to thermal instability. The helium flash, because it takes place in non-relativistic material, is more likely to reach explosive proportions.

When the value of γ falls below $4/3$ throughout a sufficient amount of the star, it will become dynamically unstable. One may easily show that the sum of the internal and gravitational energies decreases for a perturbation with a uniform contraction when the value of $\frac{\int \gamma(P/\rho) dm}{\int (P/\rho) dm}$ falls below $4/3$. The rest of the energy is converted into the kinetic energy of the perturbation. This is discussed by Ledoux (1958). Basically, the pressure cannot increase enough to maintain hydrostatic equilibrium if the star begins to contract. Any process which absorbs energy and does not increase the pressure proportionately will lower γ ; this may be seen by its explicit formulation.

$$\gamma = \left[\left(P + \frac{\partial E}{\partial v} \right) \frac{\partial P / \partial T}{\partial E / \partial T} - \frac{\partial P}{\partial v} \right] v / P$$

(The independent variables are the temperature and specific volume).

Fowler and Hoyle (1960) also proposed the decomposition of iron into helium and neutrons in massive stars as the cause of type II supernovae. Each iron nucleus need 124 MeV for the decomposition which takes place over a relatively small temperature range. The value of γ becomes as low as .8; this mechanism works so well that the core of the star collapses faster than the envelope. Investigations of the collapse have been carried out by Colgate and White (1966) and Arnett (1967). Unless the collapse is reversed by rotation, the star collapses until the central density becomes as large as 10^{15} gm/cc. At these densities nuclear interactions affect the equation of state. Arnett found that large mass stars (8 and 32 solar masses) lost energy after the collapse was stopped primarily by muon-type neutrinos; these could not interact with the material in the envelope, and no mass was ejected. Lower mass stars (2 and 4 solar masses) lost energy by electron-type neutrinos; these were caught in the envelope, and in both cases about 1.5 solar masses were ejected from the star.

Another cause of dynamic instability is the formation of electron-positron pairs, a significant number of

which exist in equilibrium with the original electrons at high temperatures and low densities. The effect of pair formation on the equation of state is discussed in Fowler and Hoyle (1964). The essential feature is that at the relevant temperatures ($T_0 = 1-3$) about two or three times as much energy is absorbed in creating the rest mass of the pairs as in forming their kinetic energy; the additional pressure created is proportional only to the latter. Radiation pressure (for which by itself $\gamma = 4/3$) dominates ion pressure and the pressure of the original electrons at low densities. The effect of the pairs is to push γ below $4/3$. At low temperatures the number of pairs decreases exponentially while the radiation pressure varies only as the fourth power of the temperature. At high temperatures the pressure of the pairs is about the same as that of the radiation; however their rest mass becomes less significant. The effect on γ then is most important at intermediate temperatures. The boundary of the "unstable area" (i.e., where γ is less than $4/3$) reaches a maximum density of about 7×10^5 gm/cc at a temperature $T_0 = 2.8$ (see Figure 1).

Rakavy and Shaviv (1966) showed that stars of more than about thirty solar masses would become dynamically unstable due to the pair formation. As the star collapses , the temperature and density increases, and eventually material near the center emerges from the un-

stable area on its high temperature boundary. The resulting stiffening of the star halts the collapse, and it rebounds. If the star is sufficiently massive the length of the path in the unstable area is long enough so by the time the collapse has been reversed, oxygen is burning at an explosive rate. The energy release is enough to disrupt all or part of the star and to eject the material with high velocities. The explosions of 45, 52, and 60 solar mass stars are investigated in this paper.

Two of the problems are the numerical techniques used in calculating the hydrodynamics and the effects of convective instability. The usual method of dealing with the hydrodynamics is an explicit scheme in which the acceleration during the time step is made proportional to a force term known at the beginning of the step. The difference equations are then stable only if the time step is less than the Courant limit; this is the time it takes sound to cross a mass zone. For comparatively slow evolution, conditions change only slightly during a time step restricted by the Courant limit; it is then preferable to take larger steps. This may be done by an implicit hydrodynamics scheme which is used here. The way in which quantities including the force are averaged over the time step is allowed to vary. One of the special cases reduces

the hydrodynamics to hydrostatic equilibrium; this is used when appropriate.

For slow evolution the effect of convective instability is to produce essentially a zero entropy gradient and perfect mixing throughout the convective zone. This no longer holds true as the evolution is speeded up. For example, the convective turbulence tends to be more efficient at convecting energy (which is roughly proportional to the third power of the speed of the turbulence) than it is in diffusing new material into the area where energy generation is taking place most strongly (proportional to the first power). The result is that the strongly burning areas tend to run out of fuel. For very fast evolution the effects of the convection may not be immediately important. However, once the turbulence and convective energy flux have been set up, they take some time to decay and may affect conditions at a later stage of the evolution. A dynamic model of the convection is derived from the equations of motion and then incorporated into the difference equations.

Chapter 2

DIFFERENCE EQUATIONS

2.1. Equations of Motion

The equations of motion and of energy conservation under spherical symmetry are

$$(1) \partial U / \partial t = -4\pi R^2 \partial P / \partial M - GM/R^2$$

$$(2) \partial E / \partial t + P \partial v / \partial t = \epsilon - \partial F / \partial M$$

where

U = radial velocity

R = radius

P = pressure

E = internal energy per unit mass

v = specific volume

ϵ = rate of energy generation per unit mass

F = total flux of energy across the spherical surface at R

The flux due to radiation is

$$-16\pi^2 a c R^4 (\partial W^4 / \partial M) / 3k$$

where

W = temperature

k = opacity

The independent variables are M, the total mass interior to the point, and the time, t. As Lagrangian co-ordinates are used, the time derivatives follow the motion of the matter.

2.2. Finite Difference Approximations

In the numerical calculation of the evolution the star is divided into N mass zones. The velocity and the radius are defined at the boundaries of the zones. The specific volume, temperature, pressure, energy and rate of energy generation are defined at the midpoints of the zones. The midpoints are denoted by half-integers; the boundaries, by integers. The size of the time step is $DT (= t^{n+1} - t^n)$. The mass of the zone centered at $I-\frac{1}{2}$ is $DM(I-\frac{1}{2})$; the mass interior to I is $M(I)$. We define

$$DM(I) = .5 \left[DM(I-\frac{1}{2}) + DM(I+\frac{1}{2}) \right]$$

The specific volume at $I-\frac{1}{2}$ is

$$v(I-\frac{1}{2}) = 4\pi \left[R(I)^3 - R(I-1)^3 \right] / 3 DM(I-\frac{1}{2})$$

The pressure at $I-\frac{1}{2}$ at time t^{n+1} is $P(I-\frac{1}{2})$; its value at t^n is $PO(I-\frac{1}{2})$. Its average value over the time step is denoted by $\langle P(I-\frac{1}{2}) \rangle$. A similar notation is used for other variables. The thermal flux is

$$F(I) = 32\pi^2 acR(I)^4 \left[W(I-\frac{1}{2})^4 - W(I+\frac{1}{2})^4 \right] / \left\{ 3 DM(I) \left[k(I-\frac{1}{2}) + k(I+\frac{1}{2}) \right] \right\}$$

Equations (1) and (2) are then approximated by

$$(3) \quad DU(I)/DT = 4\pi \langle R(I)^2 \rangle \left[\langle P(I-\frac{1}{2}) \rangle - \langle P(I+\frac{1}{2}) \rangle \right] / DM(I) - G M(I) \langle 1/R(I)^2 \rangle$$

$$(4) \quad DE(I-\frac{1}{2}) + \langle P(I-\frac{1}{2}) \rangle Dv(I-\frac{1}{2}) =$$

$$DT \left\{ \epsilon(I-\frac{1}{2}) + \left[\langle F(I-1) \rangle - \langle F(I) \rangle \right] / DM(I-\frac{1}{2}) \right\}$$

where the symbol D indicates a finite difference, e.g.,

$$DU(I) = U(I) - UO(I)$$

The usual method of defining the averaged value of a variable is as follows:

$$\langle U(I) \rangle = \alpha_1 U(I) + (1 - \alpha_1) UO(I)$$

where

$$R(I) = RO(I) + DT \langle U(I) \rangle$$

$$\langle P(I-\frac{1}{2}) \rangle = \alpha_2 P(I-\frac{1}{2}) + (1 - \alpha_2) PO(I-\frac{1}{2}) + Q(I-\frac{1}{2})$$

$$\langle F(I) \rangle = \alpha_3 F(I) + (1 - \alpha_3) FO(I)$$

$$\epsilon(I-\frac{1}{2}) = \alpha_4 \epsilon(I-\frac{1}{2}) + (1 - \alpha_4) \epsilon o(I-\frac{1}{2})$$

$$0 \leq \alpha_1, \alpha_2, \alpha_3, \alpha_4 \leq 1$$

$Q(I-\frac{1}{2})$ is the artificial viscosity used to handle shock waves (Richtmyer, 1957).

2.3. Treatment of the Surface and Center

The basic interest was in processes taking place in the interior of the star; therefore conditions at the surface were not treated precisely. The surface is defined by zero pressure. We define

$$\langle P(N+\frac{1}{2}) \rangle = 0$$

$$DM(N) = .5 DM(N-\frac{1}{2})$$

Then (3) may be used at the surface. The optical depth of the last zone was large. The surface temperature can then be neglected in forming the derivative of W^4 . The surface luminosity becomes

$$F(N) = 16\pi^2 \alpha c R(N)^4 W(N - \frac{1}{2})^4 / 3k(N - \frac{1}{2}) DM(N)$$

The center is defined by zero radius and velocity.

2.4. Conservation of Energy

The value for each α and the way in which R^2 and $1/R^2$ are averaged must first of all be determined by stability. Once stability is ensured, one would like the equations to be as accurate as possible. Ordinarily a time-centered definition (i.e., $\alpha = .5$) should be more accurate. Another guide is to ensure that conserved quantities do not change when these are now defined in a reasonable manner from the finite number of points where conditions are known. The mass is automatically conserved in a Lagrangian formulation, and the momentum in a spherically symmetric body is always zero. This leaves the total energy; conservation of energy is particularly important when the internal and gravitational energy in the star almost balance. The total energy is defined as

$$(5) E_T = \sum_{I=1}^N \left[DM(I - \frac{1}{2}) E(I - \frac{1}{2}) + .5 DM(I) U(I)^2 - GDM(I)M(I)/R(I) \right]$$

The following is to be satisfied.

$$(6) E_T(n+1) - E_T(n) = DT \left[\sum_{I=1}^N DM(I - \frac{1}{2}) \langle \epsilon(I - \frac{1}{2}) \rangle - F(N) \right]$$

If α_1 is .5, the change in kinetic energy at I over the time step is

$$.5 [U(I)^2 - U_0(I)^2] = DR(I) DU(I) / DT$$

It is then easily shown that (6) is satisfied if

$$(7) \quad \langle R(I)^2 \rangle = \frac{[R(I)^3 - R_0(I)^3]}{[3 DR(I)]} \\ = \frac{[R(I)^2 + R(I) R_0(I) + R_0(I)^2]}{3}$$

$$(8) \quad \langle 1/R(I)^2 \rangle = \frac{[1/R_0(I) - 1/R(I)]}{DR(I)} \\ = 1/[R(I) R_0(I)]$$

In the case that α_1 is not .5 the kinetic energy difference at I is

$$DR(I) DU(I) / DT + (.5 - \alpha_1) DU(I)^2$$

When relations (7) and (8) are used in this more general case the change of the total energy in excess of the right hand side of (6) is

$$\sum_{I=1}^N (.5 - \alpha_1) DM(I) DU(I)^2$$

When α_1 is less than .5 the energy increases by too large an amount, and when it is greater than .5, the energy is smaller than it should be. The former case indicates among other things that the equations are probably unstable. It will be seen that the best value is usually slightly greater than .5.

2.5. Stability

While the stability of the non-linear equations cannot be theoretically predicted, the stability of their linearized forms serves as a guide as to the stability of the former. The simplest linearization of the equations

of motion is that for sound waves. A stability analysis of these suggest that (3) and (4) will be stable if both α_1 and α_2 are equal to or greater than .5 . This appeared to be approximately the case when the non-linear equations were tested, including heat flow and energy generation. The values of α_1 , α_2 , α_3 , and α_4 were all made .5, and tests were made under a number of dynamic as well as essentially hydrostatic conditions. The equations were marginally stable. Perturbations and irregularities continued for a considerable number of time steps with about the same magnitude. Except for the case of fast motion (i.e., at the speed of sound or greater) the time steps were significantly larger than the Courant limit. When α_1 and α_2 were increased slightly the irregularities smoothed out. The value of α_1 and α_2 usually used was .51.

2.6. Hydrostatic Equilibrium

In a difference equation the change in a variable A is usually given by

$$(9) \quad DA/DT = \alpha (\partial A / \partial t)^{n+1} + (1-\alpha) (\partial A / \partial t)^n$$

where the derivatives on the right hand side are evaluated at t^{n+1} and t^n respectively. For time steps much larger than the relaxation time (appropriate only when A is approximately in equilibrium) the left hand side is much smaller than the terms making up $\partial A / \partial t$. Providing the value of $(\partial A / \partial t)^n$ is sufficiently small, the solution of equation (9) is then approximately the equilibrium value for A, as

$(\partial A / \partial t)^{n+1}$ is effectively set equal to zero. In general the derivative at t^n may not be small (for example, when A is approaching equilibrium); therefore for large time steps α must be 1. The dynamic equation (9) then reduces effectively to the equilibrium case for these large time steps.

In equation (3) the averages of the square of the radius and its inverse are redefined by

$$\begin{aligned} \langle R(I)^2 \rangle &= \alpha_5 R(I)^2 + (1 - \alpha_5) [R(I)^2 + R(I)RO(I) + RO(I)^2] / 3 \\ \langle 1/R(I)^2 \rangle &= \alpha_5 / R(I)^2 + (1 - \alpha_5) / R(I)RO(I) \end{aligned}$$

When $\alpha_5 = 0$ they return to their previous definitions, which are appropriate for the hydrodynamics case. When α_2 and α_5 are both 1, the change in the velocity is made proportional to the force at t^{n+1} ; this is the appropriate form for hydrostatic equilibrium which is used for slow evolution.

Since it is preferable to have a time-centered definition of the pressure in the energy equation, its average value in (4) is now defined separately as

$$(10) \quad \langle PE(I - \frac{1}{2}) \rangle = \alpha_6 P(I - \frac{1}{2}) + (1 - \alpha_6) PO(I - \frac{1}{2}) + Q(I - \frac{1}{2})$$

where α_6 is usually made .5 for hydrostatic equilibrium.

As long as the change in the pressure is continuous (no shock waves) the left hand side of (2) is TdS/dt . The error for $\int TdS$ in (4) is $\int Pdv - \langle PE(I - \frac{1}{2}) \rangle Dv(I - \frac{1}{2})$. By expanding the pressure in a power series this is estimated to be $-(d^2P/dv^2)(Dv)^3/12$ (for $\alpha_6 = .5$). For a fractional change in the density of 5% and 10% the error in

the entropy is of the order of one part in 10^5 and 10^4 respectively.

2.7. Method of Solution

Let the values of (3) and (4) be E_1 and E_2 when all terms are on the left hand side. The following set of equations are to be solved.

$$(11) \quad E_1(I) = 0 \quad , \quad E_2(I) = 0 \quad \quad I = 1, N$$

($E_2(I)$ is the energy equation at $I - \frac{1}{2}$). There are two independent variables at each point, for example, the velocity and the temperature (at $I - \frac{1}{2}$). The radius is given by the velocity, and the specific volume by the two neighboring radii. The solution is by a linearization procedure, so the independent variables chosen should be those in which the equations are reasonably linear.

The equations at I depend on the variables at 3 or 4 points. We denote the independent variables at I by $W_1(I)$ and $W_2(I)$ and the changes in their values (the unknowns) by $DW_1(I)$ and $DW_2(I)$. In the more general case (dependence on 4 points) the linearization gives

$$(12) \quad E(I) + A_1(I)DW(I-2) + A_2(I)DW(I-1) + A_3(I)DW(I) \\ + A_4(I)DW(I+1) = 0$$

where
$$E(I) = \begin{vmatrix} E_1(I) \\ E_2(I) \end{vmatrix} \quad \text{and} \quad DW(I) = \begin{vmatrix} DW_1(I) \\ DW_2(I) \end{vmatrix}$$

A_1, A_2, A_3 , and A_4 are 2×2 matrices; the value of the element of A_1 in the first row and column is $\partial E_1(I) / \partial W_1(I-2)$. The other elements are defined similarly. $E_1(I)$ and $E_2(I)$

are the (known) values of the equations found by the given values of the variables.

The solution consists of inverting an NxN matrix (whose elements are the 2x2 matrices) where each row has only four non-zero elements centered near the diagonal. This is done basically the same way as for the case of three non-zero elements (Richtmyer, 1957).

It is assumed that

$$(13) \quad DW(I+1) = B(I+1) + C3(I+1)DW(I) + C2(I+1)DW(I-1)$$

This is substituted into (12), and B(I), C3(I), and C2(I) are solved. Let

$$(14) \quad D(I) = [A3(I) + A4(I)C3(I+1)]^{-1}$$

$$\text{Then } B(I) = -D(I) [E(I) + A4(I)B(I+1)]$$

$$C3(I) = -D(I) [A2(I) + A4(I)C2(I+1)]$$

$$C2(I) = -D(I) A1(I)$$

Relation (13) exists for the equations centered at N.

The procedure works down from N to 1 where $DW(1) = B(1)$.

The procedure then works back up to N, giving $DW(I)$ at

each point. The linearization is iterated until (11)

converges to a sufficient degree of accuracy.

As the equations are at times rather non-linear, the linearization did not always work, and supplementary procedures had to be added. They consist basically in limiting the size B(I) and DW(I) may take.

2.8. The Treatment of Energy Generation

With nuclear reactions present, equations (1) and (2) must be supplemented by the rate of change of each isotope. In the simplified version of reactions considered here the reaction chain has no loops. In that case in a finite difference scheme one "sweep" along the chain gives the change in each mass fraction. For each isotope (j) the rate of change of its mass fraction, X_j , is

$$(15) \quad \partial X_j / \partial t = XP_j - \epsilon_j / Q_j$$

where XP_j is the rate of production of the isotope (determined by reaction rates farther down on the chain), and Q_j is the energy released by a unit mass reacting via ϵ_j .

The finite difference approximation is

$$(16) \quad DX_{j(I-\frac{1}{2})} / DT = XP_{j(I-\frac{1}{2})} - \langle \epsilon_{j(I-\frac{1}{2})} \rangle / Q_j$$

The quantity $XP_{j(I-\frac{1}{2})}$ is known when the isotopes are solved for in the right order. One method used to define $\langle \epsilon_{j(I-\frac{1}{2})} \rangle$ was the following; ϵ_j is usually the product of X_j to some power ν and a function f depending on the specific volume and temperature.

$$\epsilon_j = X_j^\nu f(v, w)$$

Denoting by $X_{j(I-\frac{1}{2})}$, $X_{j(I-\frac{1}{2})}$, $f(I-\frac{1}{2})$, and $f_{o(I-\frac{1}{2})}$ the values of X_j and f at t^{n+1} and t^n respectively, we define

$$(17) \langle \epsilon_{j(I-\frac{1}{2})} \rangle = X_{j(I-\frac{1}{2})} \chi_{0(I-\frac{1}{2})j}^{\nu-1} \left[\alpha_4 f(I-\frac{1}{2}) + (1 - \alpha_4) f_0(I-\frac{1}{2}) \right]$$

Then $X_{j(I-\frac{1}{2})}$ may be directly solved for by (16) and (17). In solving the set of equations (11) the set of equations (16) and (17) act as definitions in giving the average rate of energy generation at $I-\frac{1}{2}$ as a function of $W(I-\frac{1}{2})$ and $\nu(I-\frac{1}{2})$. The mass fraction of each isotope automatically remains between 0 and 1.

At the densities at which investigations were carried out virtually all neutrinos escape directly from the star. Neutrino losses are then treated as a negative rate of energy generation.

Chapter 3

CONVECTION

3.1. Introduction

The general method for the derivation of the convective model is taken from Cowling (1936). At any point the velocity U is divided into a mean velocity V and a convective velocity W . The latter is defined so that it does not effect, on the average, any mass transfer. (For the case of spherical symmetry the averaging is done by integrating over a spherical shell).

$$(1) \overline{\rho U_i} = \overline{\rho V_i} + \overline{\rho W_i} = \overline{\rho} V_i \quad i=1,2,3$$

V_i remains constant over the area of averaging. By this definition the convective velocity does not possess any average momentum. It is also possible to divide the kinetic energy into the energy of the mean motion and of the convective turbulence, the latter being, in a sense, a form of internal energy.

$$(2) \frac{1}{2} \overline{\rho U_i U_i} = \frac{1}{2} \overline{\rho V_i V_i} + \frac{1}{2} \overline{\rho W_i W_i}$$

(A pair of the same indices indicates a summation).

The equations of motion are averaged in the same way. The equations for the conservation of mass, energy, and momentum are

$$(3) \frac{\partial \rho}{\partial t} + \nabla_i (\rho U_i) = 0$$

$$(4) \quad \frac{\partial(\rho E)}{\partial t} + \nabla_i(\rho E U_i) + P \nabla_i U_i = \rho \dot{e} - \nabla_i F_i - P_{ij} \nabla_j U_i$$

$$(5) \quad \frac{\partial(\rho U_i)}{\partial t} + \nabla_j(\rho U_i U_j) = \rho G_i - \nabla_i P - \nabla_j P_{ij}$$

P_{ij} is the viscosity stress tensor; G_i is the externally applied force. Equation (5) may also be written

$$(6) \quad \rho \left[\frac{\partial U_i}{\partial t} + U_j \nabla_j U_i \right] = \rho G_i - \nabla_i P - \nabla_j P_{ij}$$

When averaged (3) becomes

$$(7) \quad D\bar{\rho}/Dt = -\overline{\rho \nabla_j V_j}$$

where

$$D/Dt = \partial/\partial t + v_j \nabla_j$$

, i.e., a Lagrangian derivative following the mean motion.

The left hand side of (4) may be written

$$D(\rho E)/Dt + \rho E \nabla_j V_j + \nabla_j(\rho E W_j) + P \nabla_j V_j + P \nabla_j W_j$$

and when averaged it becomes

$$(8) \quad \overline{\rho} D(\overline{\rho E}/\overline{\rho})/Dt + \overline{\rho} \overline{P} D\bar{v}/Dt = -\overline{\nabla_j(\rho E W_j)} - \overline{P \nabla_j W_j} + \overline{\rho \dot{e}} - \overline{\nabla_j F_j} - \overline{P_{ij} \nabla_j U_i}$$

The basic difference of (8) with (4) is the convective energy flux, $\overline{\rho E W_j}$. It will be seen that the second term on the right hand side usually acts to reinforce the convective flux. The viscosity term largely

represents heat formed by the decay of the turbulent kinetic energy. Its approximate value is given later on.

Neglecting the effect of viscosity on the mass motion, equation (5) becomes

$$(9) \quad \bar{\rho} DV_i/Dt = \bar{\rho} G_i - \bar{\nabla}_i P - \bar{\nabla}_j \rho W_i W_j$$

For spherical symmetry the radial component is

$$(10) \quad \bar{\rho} DV_r/Dt = \bar{\rho} G_r - \partial \bar{P} / \partial r - [\partial (r^2 \overline{\rho W_r^2}) / \partial r - r \overline{\rho W_\theta^2} - r \overline{\rho W_\phi^2}] / r^2$$

It will be assumed that the distribution of the kinetic energy of the turbulence is approximately isotropic, i.e.,

$$\overline{\rho W_r^2} = \overline{\rho W_\theta^2} = \overline{\rho W_\phi^2}$$

In that case the Reynolds stresses act as a pressure-like term.

$$(11) \quad \bar{\rho} DV_r/Dt = \bar{\rho} G_r - \partial (\bar{P} + \overline{\rho W_r^2}) / \partial r$$

The rate of formation of the kinetic energy of the mean motion is

$$(12) \quad \bar{\rho} D(\frac{1}{2} V_r^2) / Dt = \bar{\rho} G_r V_r - V_r \partial (\bar{P} + \overline{\rho W_r^2}) / \partial r$$

3.2. Treatment of the Turbulent Energy and Energy Flux

In addition to the usual equations of motion we need the time rate of change of the turbulent kinetic energy and of the convective energy flux. Two assumptions are made. One is that the density fluctuations over any spherical surface caused by the convection are small.

Another is that the pressure remains constant over the area of averaging or at least that it is not correlated with (the radial component of) the convection so that it may be averaged separately.

The energy flux is roughly proportional to the averaged convective velocity.

$$\begin{aligned}
 (13) \quad L_i &\equiv \overline{\rho E W_i} = \overline{\rho W_i \left[\bar{E} + \left(\frac{\partial E}{\partial \rho} \right)_P (\rho - \bar{\rho}) + \right.} \\
 &\quad \left. \left(\frac{\partial E}{\partial P} \right)_\rho (P - \bar{P}) \right]} \\
 &= \overline{\left(\frac{\partial E}{\partial \rho} \right)_P \rho W_i (\rho - \bar{\rho})} = \overline{\left(\frac{\partial E}{\partial \rho} \right)_P \rho^2 W_i} \\
 &\approx - \overline{\left(\frac{\partial E}{\partial \rho} \right)_P \bar{\rho}^2 W_i}
 \end{aligned}$$

To the extent the pressure is correlated with the convection the derivative becomes

$$\overline{\left(\frac{\partial E}{\partial \rho} \right)_P} \rightarrow \overline{dE/d\rho} = \overline{\left(\frac{\partial E}{\partial \rho} \right)_P} + \overline{\left(\frac{\partial E}{\partial P} \right)_\rho} \overline{dP/d\rho}$$

Contracting equations (5) and (6) with U_i and adding gives the rate of change of the total kinetic energy.

$$\begin{aligned}
 &D(\frac{1}{2} \overline{\rho U_i U_i})/Dt + \frac{1}{2} \overline{\rho U_i U_i \nabla_j V_j} + \frac{1}{2} \overline{\nabla_j (W_j \rho U_i U_i)} \\
 &= \overline{U_i \rho G_i} - \overline{U_i \nabla_i P} - \overline{U_i \nabla_j P_{ij}}
 \end{aligned}$$

The derivative of the energy of the mean motion is subtracted, leaving that of the convective turbulence. The term involving the external force is neglected.

$$(14) \quad \overline{\rho} \frac{D}{Dt} \left(\frac{1}{2} \overline{\rho W_i W_i / \bar{\rho}} \right) = - \overline{W_i \nabla_i P} - \overline{W_i \nabla_j P_{ij}}$$

$$-\frac{1}{2} \overline{\nabla_j (w_j \rho^{w_i w_i})} - \overline{\rho^{w_i w_j} \nabla_j v_i}$$

The first term on the right is the basic driving force. The term $\overline{\rho^{w_i}}$ may be added to it, and under hydrostatic equilibrium it becomes $g \overline{w_i \Delta \rho}$. It is seen that the turbulent kinetic energy is created by "buoyancy forces", i.e., the differential acceleration the pressure gradient has on elements of varying density. Whether or not the buoyancy effect acts to increase or decrease the turbulence depends on how the density fluctuations are correlated with the convective velocity. This, of course, ultimately depends on whether or not the material is convectively unstable. From (13) this effect is proportional to the energy flux.

The second term is the dissipation by the viscosity. From the study of homogeneous turbulence this has been shown to be approximately $\overline{\rho |w|^3} / \ell$; ℓ is roughly the length of those eddies which have the maximum kinetic energy (Batchelor, 1953). This is valid when these eddies have a large Reynolds number which is ordinarily true for the conditions under consideration. Under these conditions, to a first approximation, the turbulent spectrum may be divided into two groups. One group, with a characteristically small wave number, is dominated by inertial forces and contains most of the kinetic energy. The second group, with a larger wave number, has a Reynolds num-

ber of the order of one. The large eddies (the first group) do not directly convert their energy into heat; it is instead transferred to the smaller eddies. The small eddies, for which viscosity is important, are roughly in equilibrium, converting kinetic energy into heat as fast as they receive it from the large eddies. Even if the turbulence is not homogeneous at the scale of the large eddies, it should be at the smaller scale, and the dissipation rates should remain about the same.

The factor λ is more or less the equivalent of a mixing length. Since the larger the eddy the slower it decays, λ should be about the size of the (smallest) characteristic length of the system as we would expect that the largest eddies formed would be of this magnitude. For convection in a stellar atmosphere the mixing length is often taken equal to a scale height. However the eddy size can hardly be larger than the radius, which near the center is less than a scale height. The procedure adopted was to make λ proportional to the minimum of the pressure scale height, the radius, and the length of the convective zone itself. The constant of proportionality can be changed to determine what effect this might have on the evolution of the system.

The third term represents the diffusion of the convective energy. It tends to spread out the turbulence evenly; it also introduces it to regions previously stable.

It disappears when integrated over the entire convective zone. In estimating its magnitude the derivative can be replaced by $1/\ell$, since the energy should not change substantially in a smaller distance.

$$\begin{aligned} |\overline{\nabla_j (w_j \rho w_i w_i)}| &\leq \overline{|\rho w_r (\overline{|w|^2} + 2 \Delta w \overline{|w|})|} / \ell \\ &= O(\overline{|\Delta \rho|} \overline{|w|^3} / \ell) \end{aligned}$$

As the term is small compared to the dissipation it is, for simplicity, neglected here. However, if one is interested in determining how far the turbulence extends beyond the convectively unstable region, this term must be retained. Here it will be assumed that the turbulence effectively stops at the edge of the convectively unstable zone (except for decaying turbulence in a previously convectively unstable region). Another effect of the diffusion is to transport energy from the area where the turbulence is produced most vigorously to the fringes of the turbulent area. However as long as the speed of the convection is small compared to the speed of sound, this effect will be considerably smaller than the flux of internal energy ($L \approx \overline{|\Delta \rho|} \overline{|w|} E$).

For isotropic turbulence the last term is

$$-\overline{\rho} \overline{\rho w_r^2} D\overline{v}/Dt$$

For $\overline{w_r}$ we substitute its value as given by (13) and equation (14) becomes

$$(15) \quad D(1.5 \overline{\rho w_r^2} / \overline{\rho}) / Dt = L_r (\partial \overline{P} / \partial r) / [\overline{\rho}^3 (dE/d\rho)]$$

$$- \overline{|w_r|^3} / \ell - \overline{\rho w_r^2} D\bar{v}/Dt$$

The time derivative of L_i is

$$\begin{aligned}
 (16) \quad D(\overline{\rho E w_i})/Dt &= \overline{\rho E D(U_i - V_i)/Dt} + \overline{w_i D(\rho E)/Dt} \\
 &= \underbrace{- \overline{\rho E w_j \nabla_j w_i}}_1 - \underbrace{\overline{\rho E w_j \nabla_j v_i}}_2 + \underbrace{\overline{\rho E / \rho \nabla_j (\rho w_i w_j)}}_3 \\
 &- \underbrace{\left[\overline{E \nabla_i P} - \overline{\rho E \nabla_i P / \rho} \right]}_4 - \underbrace{\left[\overline{E \nabla_j P_{ij}} - \overline{\rho E / \rho \nabla_j P_{ij}} \right]}_5 \\
 &- \underbrace{\overline{w_i \rho E \nabla_j v_j}}_6 - \underbrace{\overline{w_i E \nabla_j (w_j \rho)}}_7 - \underbrace{\overline{w_i w_j \rho \nabla_j E}}_8 \\
 &+ \underbrace{\overline{w_i P (D\rho / Dt) / \rho}}_9 + \underbrace{\overline{P w_i w_j \nabla_j \rho / \rho}}_{10} + \underbrace{\overline{\rho w_i \epsilon}}_{11} \\
 &- \underbrace{\overline{w_i \nabla_j F_j}}_{12} - \underbrace{\overline{w_i P_{kj} \nabla_j U_k}}_{13}
 \end{aligned}$$

The terms on the right hand side are numbered. Their approximate values for the radial component of the flux are given below.

Terms 1,3, and 7 combine to give

$$- \left[\overline{E \nabla_j (w_i w_j \rho)} - \overline{\rho E / \rho \nabla_j (w_i w_j \rho)} \right]$$

It reflects the fact that the Reynolds stresses tend to have a greater effect on the lighter usually more energetic elements. Similarly term 4

$$- \left[\overline{E \nabla_i P} - \overline{\rho E / \rho \nabla_i P} \right]$$

shows that the lighter elements are given a greater acceleration by the pressure gradient. The effect is usually to increase the energy flux. Both these terms are proportional to

$$\overline{E} - \overline{\rho E} / \overline{\rho} \approx -(\overline{dE/d\rho}) \overline{\Delta\rho^2} / \overline{\rho}$$

Since the square of the density fluctuations is supposed to be small, these terms will be neglected.

Terms 2 and 6 are

$$- \overline{\rho E W_r^2} 2V_r / r \quad - \overline{\rho E W_r^2} (\partial V_r / \partial r)$$

Terms 8 and 10 give

$$- \overline{\rho W_r^2} \left[\partial \overline{E} / \partial r + \overline{P} \partial \overline{v} / \partial r \right]$$

This is the entropy gradient (except for the effects of composition gradients). This is the basic driving force term that with the "buoyancy force" effect on the turbulent energy creates the convective turbulence and energy flow.

Term 9 is proportional to the rate of change of density. It is usually comparatively small and will be neglected.

Term 11 is caused by the difference in the rate of energy generation between the hot and cold elements. Since nuclear reaction rates are strongly dependent on the temperature, it may be significant in some cases. Below a certain value of the speed of convection the energy gained is greater than that lost by the mixing of hot and cool elements. Its value is

$$\overline{\rho E W_r} \quad \overline{(dE/dE)}$$

Term 12 is a dissipation effect whereby energy is radiated from hot to cool elements. Under the conditions considered here this was not important. The viscosity (terms 5 and 13) should not have an important effect on the large scale eddies which are important for the energy transport. The dissipation for the turbulent energy may be interpreted as a "mixing" of the material in a distance λ . This same estimate will be used here.

Equation (16) now becomes

$$(17) \quad D(r^2 L_r)/Dt / r^2 = - \overline{\rho W_r^2} \left[\overline{\partial E / \partial r} + \overline{P} \overline{\partial v / \partial r} \right] \\ + L_r \overline{dE/dE} - L_r \overline{|W_r|} / \lambda - 2L_r (\partial v_r / \partial r)$$

3.3. Conservation of Energy

The viscosity term in the energy equation (8) is approximated as the energy lost by the turbulence through its dissipation. Then using the approximations developed in (15) the energy equation may be rewritten as

$$(18) \quad \overline{\rho} \left[D(\overline{\rho E / \rho} + 1.5 \overline{\rho W_r^2 / \rho}) / Dt + (\overline{P} + \overline{\rho W_r^2}) \overline{Dv / Dt} \right] \\ = - (\partial r^2 L_r / \partial r) / r^2 - (\partial r^2 \overline{P W_r} / \partial r) / r^2 - (\partial r^2 \overline{F_r} / \partial r) / r^2 \\ + \overline{\rho \epsilon} \\ \approx - \frac{\partial}{\partial r} \left\{ r^2 \left[L_r (1 - \overline{P} / \overline{\rho} \overline{dE/d\rho}) + \overline{F_r} \right] \right\} / r^2 + \overline{\rho \epsilon}$$

As was mentioned before, the second term on the right hand side of (8) usually makes the effective energy flux larger.

The coefficient of L_r was generally given the value $4/3$. Adding the rate of formation of the kinetic energy of the mean motion gives

$$(19) \quad \overline{\rho} D(\overline{\rho E}/\overline{\rho} + 1.5 \overline{\rho W_r^2}/\overline{\rho} + \frac{1}{2} \overline{V_r^2})/Dt = \\ - \partial \left\{ r^2 \left[4L_r/3 + \overline{F_r} + (\overline{P} + \overline{\rho W_r^2}) \overline{V_r} \right] \right\} / \partial r \quad /r^2 \\ + \quad \overline{\rho G_r V_r} + \overline{\rho \epsilon}$$

The approximations developed do not violate the conservation of energy.

3.4. The Condition of Convective Instability

We now show that the equations developed here are consistent with and predict the condition for convective instability. Eliminating usually unimportant terms and dissipative effects, equations (15) and (17) may be written

$$D(r^2 L_r)/Dt \quad /r^2 = -\overline{\rho W_r^2} \left[\partial \overline{E} / \partial r + \overline{P} \partial \overline{v} / \partial r \right] \\ D(1.5 \overline{\rho W_r^2})/Dt = L_r (\partial \overline{P} / \partial r) / \left[\overline{\rho}^3 (dE/d\rho) \right]$$

If the pressure and entropy gradients have opposite signs, the solution is an oscillation which will decay when the dissipation is added (convective stability). If they have the same sign, the solution grows until checked by the dissipation (instability). In a star, of course, there is instability if the entropy increases toward the center. In using this approach the effect of a composition gradient

on the stability (e.g., semi-convection) does not enter explicitly.

3.5. Convective Difference Equations

The averaged speed of the convective turbulence ($\overline{|w_r|}$) and the total convective energy flux across the spherical surface ($4\pi r^2 L_r$) are defined at the boundary of each mass zone. Their values at t^{n+1} are denoted by $w(I)$ and $L(I)$ and at t^n by $w_0(I)$ and $L_0(I)$. The equations to be approximated are (11), (18), (15), and (17). Often the relaxation time for the convection is smaller than the characteristic time of the evolution of the star. The convection is then approximately in equilibrium, and as the time step used is proportional to the evolution time, the (dynamical) difference equations for the convection must reduce to the equilibrium case for these large time steps. This is done by giving all quantities on the right hand side of the difference forms of equations (15) and (17) their values at the advanced time t^{n+1} (as explained in section 2.6.).

The pressure-like term caused by the Reynolds stresses is defined at $I-\frac{1}{2}$ as $S(I-\frac{1}{2})$. This is usually given the average value

$$\langle S(I-\frac{1}{2}) \rangle = .5 [w(I-1)^2 + w(I)^2] / v(I-\frac{1}{2})$$

The term $dE/d\rho$, under typical conditions, was usually approximated by $-3Pv^2$. We define $Y(I)$ as the mean of the

value of $(\partial E / \partial \rho)_p / (\partial E / \partial \rho)_p$ defined at $I - \frac{1}{2}$ and $I + \frac{1}{2}$ at the forward time t^{n+1} . Here the symbol D indicates the (finite) change in a variable over the time step DT . The difference equations are

$$(20) \quad DU(I)/DT = -4\pi \langle R(I)^2 \rangle \left[\langle P(I + \frac{1}{2}) \rangle + \langle S(I + \frac{1}{2}) \rangle - \langle P(I - \frac{1}{2}) \rangle - \langle S(I - \frac{1}{2}) \rangle \right] / DM(I) - GM(I) \langle 1/R(I)^2 \rangle$$

$$(21) \quad DE(I - \frac{1}{2}) + \left[\langle PE(I - \frac{1}{2}) \rangle + \langle S(I - \frac{1}{2}) \rangle \right] Dv(I - \frac{1}{2}) + .75 \left[DW(I)^2 + DW(I-1)^2 \right] =$$

$$DT \left\{ \langle E(I - \frac{1}{2}) \rangle + \left[\langle 4L(I-1)/3 \rangle + \langle F(I-1) \rangle - \langle 4L(I)/3 \rangle - \langle F(I) \rangle \right] / DM(I - \frac{1}{2}) \right\}$$

Equations (20) and (21) are the new versions of (3) and (4) of the previous chapter. Note that (18) instead of (8) is used as the basis of (21). While the change in the turbulent energy is usually relatively small, the rate at which it is being produced and dissipated is quite large (and nearly cancel each other). By using (18) two large non-linear terms are replaced by two smaller relatively linear quantities, which is to be preferred in numerical work. $U(I)$ now indicates the average radial velocity.

The two convective equations are

$$(22) \quad DL(I)/DT = W(I)^2 R^2 P(I) \left\{ .5 \left[P(I - \frac{1}{2}) + P(I + \frac{1}{2}) \right] \left[v(I - \frac{1}{2}) - v(I + \frac{1}{2}) \right] + E(I - \frac{1}{2}) - E(I + \frac{1}{2}) \right\} + L(I) Y(I) - 8\pi L(I) R(I)^2 \left[U(I+1) - U(I-1) \right] / \left\{ DM(I) \left[v(I - \frac{1}{2}) + v(I + \frac{1}{2}) \right] \right\} - L(I) W(I) / \lambda(I)$$

where

$$R2P(I) = 32\pi^2 R(I)^4 / \left\{ DM(I) \left[v(I-\frac{1}{2})^2 + v(I+\frac{1}{2})^2 \right] \right\}$$

$$(23) \quad 1.5 \frac{DW(I)^2}{DT} = L(I) \left[P(I-\frac{1}{2}) - P(I+\frac{1}{2}) \right] / \left\{ 1.5 \left[P(I-\frac{1}{2}) + P(I+\frac{1}{2}) \right] DM(I) \right\} - W(I)^3 / \lambda(I)$$

$$- .5 W(I)^2 \left[(Dv(I-\frac{1}{2})/DT)/v(I-\frac{1}{2}) + (Dv(I+\frac{1}{2})/DT)/v(I+\frac{1}{2}) \right]$$

The term $\lambda(I)$ is defined within a coefficient as the minimum of the pressure scale height, the radius, and the length of the convective zone.

Energy Conservation and Stability of the Difference Equations

The total energy is redefined by adding to it the sum

$$\sum_{I=1}^N 1.5 DM(I) W(I)^2$$

The energy is then conserved to the same extent as in the previous chapter. As mentioned before, equations (22) and (23) reduce to the equilibrium form for large time steps. Using these forms of the convective equations, the stability appeared to be about the same as that of the equations omitting convection that were described in chapter 2.

Detection of Convective Instability

When there is no convection ($W(I), L(I) = 0$), equations (22) and (23) are not applied. Instability is

considered to exist at I when the term

$$.5 \left[P(I-\frac{1}{2}) + P(I+\frac{1}{2}) \right] \left[v(I-\frac{1}{2}) - v(I+\frac{1}{2}) \right] + E(I-\frac{1}{2}) - E(I+\frac{1}{2})$$

becomes positive. This is tested for at the beginning of each time step and, optionally, at several times during the convergence procedure. When instability is detected, an initial estimate is made for $L(I)$, usually by equating it to the sum of $L(I-1)$ and $\langle \epsilon(I-\frac{1}{2}) \rangle / DT$. $W(I)$ is then found through equation (23). Equations (22) and (23) are then applied at I until the turbulence has died out, which will be a number of time steps after the boundary at I has become stable again.

Diffusion Effects

When convective diffusion is added, equations (15) and (16) of the previous chapter become

$$(24) \quad DX_j/Dt = XP_j - \epsilon_j/Q_j + \left[\partial (r^2 \overline{w_r X_j}) / \partial r \right] / \bar{\rho} r^2$$

and

$$(25) \quad DX_{j(I-\frac{1}{2})}/DT = XP_{(I-\frac{1}{2})j} - \langle \epsilon_{j(I-\frac{1}{2})} \rangle / Q_j \\ + 2\pi \left\{ R(I)^2 W(I) \left[X_{j(I+\frac{1}{2})} - X_{j(I-\frac{1}{2})} \right] \right. \\ \left. + R(I-1)^2 W(I-1) \left[X_{j(I-\frac{3}{2})} - X_{j(I-\frac{1}{2})} \right] \right\} / \left[DM(I-\frac{1}{2}) v(I-\frac{1}{2}) \right]$$

The composition at $I-\frac{1}{2}$ now effectively depends on the composition of all points of the convective zone. The value

of $X_j(I-\frac{1}{2})$ does not fit in with the solution scheme which assumes dependence on only 3 or 4 neighboring points about I. $X_j(I-\frac{1}{2})$ may be solved for, using equation (23), before each new iteration, using values of the other variables as given by the previous iteration. A simpler method is to hold the value fixed during the time step, solving only at the beginning of the step. The former procedure should be more accurate; however, it usually slows down the rate of convergence.

Method of Solution

Equation (23) may be used to solve for $W(I)$ in terms of the other variables. The method of solution is the same as that outlined in the previous chapter. The only difference is that there are three equations and three independent variables at each point where convection exists.

THE EQUATION OF STATE AND RATES OF ENERGY GENERATION

4.1. Equation of State

The pressure and energy used includes the effects of radiation, ions, and electrons. The density and the pressure and energy of the electrons, including electron-positron pairs, are

$$\begin{aligned}
 (1) \rho &= \frac{8\pi m^3 c^3 \mu H}{h^3} \int_0^\infty dx x^2 \left\{ \frac{1}{[\exp(z(y-E_F)) + 1]} \right. \\
 &\quad \left. - \frac{1}{[\exp(z(y+E_F)) + 1]} \right\} \\
 (2) P &= \frac{8\pi m^4 c^5}{3h^3} \int_0^\infty dx x^4/y \left\{ \frac{1}{[\exp(z(y-E_F)) + 1]} \right. \\
 &\quad \left. + \frac{1}{[\exp(z(y+E_F)) + 1]} \right\} \\
 (3) E &= \frac{v8\pi m^4 c^5}{h^3} \int_0^\infty dx x^2 y \left\{ \frac{1}{[\exp(z(y-E_F)) + 1]} \right. \\
 &\quad \left. + \frac{1}{[\exp(z(y+E_F)) + 1]} \right\}
 \end{aligned}$$

where μ is the electron molecular weight (excluding pairs)

$$z = mc^2/kT$$

x is the momentum in terms of mc

y is the energy including rest mass in terms of mc^2

E_F is the chemical potential in terms of mc^2 , and is defined by equation (1) as an implicit function of the temperature and density.

For non-degenerate material where E_F is less than one, the denominators can be expanded, and the integral of each term of the sum may be expressed in terms of modified

Hankel functions of the second kind, giving

$$(4) \rho = \frac{8\pi m^3 c^3 \mu H}{h^3} \sum_{n=1}^{\infty} (-)^{n+1} K_2(nz)/nz \left[\exp(nzE_F) - \exp(-nzE_F) \right]$$

$$(5) P = \frac{8\pi m^4 c^5}{3h^3} \sum_{n=1}^{\infty} (-)^{n+1} 3K_2(nz)/n^2 z^2 \left[\exp(nzE_F) + \exp(-nzE_F) \right]$$

$$(6) E = \frac{v8\pi m^4 c^5}{h^3} \sum_{n=1}^{\infty} (-)^{n+1} \left[3K_2(nz)/n^2 z^2 + K_1(nz)/nz \right] \left[\exp(nzE_F) + \exp(-nzE_F) \right]$$

For z greater than 5 the Hankel functions may be accurately expressed by the first several terms of their asymptotic expansions. For z between 1 and 5 the following expressions give the functions better than one part in 10^4 .

$$(7) K_2(z) = \exp(-z) (\pi/2z)^{\frac{1}{2}} (1 + 15/8z) + 2 \exp \left[-z(.95851 z^2 + 14.122 z + 14.267)/(z^2 + 10.957 z + 3.4912) \right] / z^2$$

$$(8) K_1(z) = \exp(-z) (\pi/2z)^{\frac{1}{2}} + \exp \left[-z(1.0103 z^2 + 7.5624 z + 6.1486)/(z^2 + 5.2018 z + 1.3085) \right] / z$$

The general method of determining the electron pressure and energy was to interpolate between tabulated values. The actual (linear) interpolation was in each tabulated variable divided by appropriate powers of the density and temperature, each power chosen so the interpolated quantity varied slowly. Because of the high temperature dependence of the pressure and energy where pair-production was important, this method was not found to be satisfactory, if the number of points in the tables were to be kept within a reasonable limit. The method used here was to tabulate the difference between the chemical potential (solved by iterating (4)) and the "first order" potential (the value when only the first term of the sum in (4) is kept). The first order chemical potential is easily determined, and the difference was usually small enough so its value found by linear interpolation was sufficient. Once the potential is known, the pressure and energy are given by the first few terms of the sums in (5) and (6).

4.2. Nuclear Reactions

Important reactions include oxygen burning in which silicon is taken as the chief end product. The rate of energy production is (Fowler and Hoyle, 1964)

$$(9) \quad \log \epsilon_o = 55.7 + \log(\rho X_o^2) - 2/3 \log T_9 \\ - 59.04 (1/T_9 + .080)^{\frac{1}{3}} \quad \text{ergs/gm-sec}$$

The energy per reaction is 16.5 MeV.

By the alpha process silicon is converted largely to Ni⁵⁶. The rate is determined by the breakup of Mg²⁴, a small amount of which exists in equilibrium with the silicon. The rate was found to be (Finzi and Wolf, 1966)

$$(10) \log \epsilon_{Si} = 30.47 + \log X_{Si} - 1/7 \log(1/X_{Si} - 1) \\ + 6.31 \log(T_9/3) - 61.67/T_9 \quad \text{ergs/gm-sec}$$

The energy release per gram of material is 1.5×10^{17} ergs.

4.3. Neutrino Losses

For non-degenerate material at elevated temperatures the major losses are due to pair-annihilation and the photo-neutrino process. The former predominates for temperatures above $T_9 = .5$. The non-degenerate non-relativistic rates are (Levine, 1963)

$$(11) \epsilon_{pa.} = .49 \times 10^{19} T_9^3 \exp(-118.6/T_9) / \rho \quad \text{ergs/gm-sec}$$

$$(12) \epsilon_{pn.} = 1.0 \times 10^8 T_9^8 / \mu \left[1 + 1.04 \times 10^{12} T_9^3 \exp(-118.6/T_9) / \rho^2 \right]^{\frac{1}{2}} \\ \text{ergs/gm-sec}$$

For T_9 greater than .5, values for the loss due to pair-annihilation were determined by interpolating, using the table given by Chiu (1961). The last coefficient in equation (12) (photo-neutrino losses) is to include the effects of the extra particles due to pair formation.

Plasmon neutrino losses are important only at high densities, where the material is degenerate.

4.4 Opacity

The opacity used was

$$(13) \kappa = \left[.38/(1+T_9) + 4.6 \times 10^{-7} \langle Z^2/A \rangle \rho / T_9^{3.5} \right] / \mu$$

The first term is due to electron scattering, and the second is bound-free absorption (Schwarzschild, 1958). The important term was the electron scattering. The coefficient $1/(1+T_9)$ is a relativistic correction. Equation (13) is only appropriate for non-degenerate material. For degeneracy the effective opacity becomes much smaller, and is determined largely by the heat conduction of the degenerate electrons. For the opacity the definition of the electron molecular weight, μ , must include the pairs. This means that at low densities the opacity is much larger than would otherwise be the case.

Chapter 5

EXPLOSIONS OF 45, 52, AND 60 SOLAR MASS MODELS

5.1. Initial Models

The initial models were approximately isentropic with a central temperature $T_0 = .7$. The density gradient was determined by making $(\partial v / \partial P)_s / (dv/dP)$ a constant, C_1 , throughout the star. Table 1 gives properties of the initial models.

The composition chosen was pure oxygen throughout the star. At a central temperature of roughly $T_0 = .5$, neutrino losses begin to dominate loss of energy through radiation. Unless the oxygen core (for stars in this mass range helium is converted mostly into oxygen) already extends throughout most of the star, helium will begin to burn at its edge as the star contracts. The energy generation will grow until it approximately equals the neutrino losses. As evolution is proceeding too fast for much energy to be lost by radiation, most of it goes into raising the entropy of the material outside the core (neutrino losses being concentrated near the center). The convective zone formed should extend most of the way to the surface, and so most of the star will be converted into oxygen. This extension of the convection nearly to the surface for shell burning should be a common feature of the evolution when neutrino losses predominate. If there is a substantial envelope of helium or hydrogen,

Table 1

Mass	Central Specific Volume (cc/gm)	Total Energy (ergs)	C1	Number of ** Mass Zones
45	1.185 E-4 *	-2.38 E51	.995	50
52	1.267 E-4	-2.73 E51	.980	50
60	1.416 E-4	-3.17 E51	.995	50

* The term E-4 indicates the preceding factor is to be multiplied by 10^{-4} .

** The number of (equal mass) zones used was the smallest number for which it was felt would give reasonable results. As neither a smaller nor larger number of zones was used in the evolutionary calculations, it is not known how sensitive the results depend on the number of the zones.

the masses given here refer to the mass of the core, since the low molecular weight envelope should be sufficiently extended so as to not significantly affect conditions near the center (see Remarks).

For stars of sufficient mass the entropy near the center is high enough that, when the central temperature reaches $T_0 = 1.5-2.0$, the material near the center penetrates the "unstable area" (i.e., where γ is less than $4/3$) caused by the production of electron-positron pairs (see Figure 1). The material approaches this area at a very oblique angle, as its boundary almost follows a line of constant entropy. Eventually the pressure does not increase sufficiently to continue to support the star as it slowly contracts, and it begins to collapse. Whether or not the star becomes dynamically unstable, the extent of the collapse if it does, and the intensity of the possible resulting explosion, depends heavily on the entropy near the center. For this reason the size of the explosion is probably fairly sensitive to the initial conditions chosen. For the same reason it is also sensitive whether or not neutrino losses are included (they are included here). When they are included, the entropy gradient of about the outer half of the star is frozen in. In the

interior an increasingly large entropy gradient is created near the center where the losses are concentrated. Because of the relatively low entropy near the center, the length of the path of the material through the unstable area is smaller. As soon as enough material emerges on the high temperature side of the unstable area, the stiffening effect starts to reverse the collapse. The inclusion of neutrino losses should then reduce the intensity of the explosion.

Because of the probable sensitivity on initial conditions more realistic starting conditions should give somewhat different results. However, the masses and initial conditions used cover most of the range of the intensities of the explosions; this range of the intensities was the basic feature of interest.

5.2. Onset of Instability

From a central temperature $T_0 = .7$, the models took roughly 100 years to reach the point of instability. Over this period neutrino losses increased by more than a factor of 10^4 . At the end evolution was quite fast, on the order of a day or less. As the net energy of the star is roughly proportional to the inverse of the radius, the average inward velocity should be proportional to the neutrino loss rate. The onset of instability was determined when the (logarithmic) rate of change of the kinetic energy was observed to be much larger than the correspon-

Table 2 M = 45

Mass Fraction X_r	volume (cc/gm) v	Temperature T_9	$(\partial \log P / \partial \log \rho)_s$ γ	neutrino losses (ergs/gm-sec) ϵ_ν
.01	.253 E-5	1.95	1.338	.166 E13
.03	.339 E-5	1.89	1.328	.154 E13
.11	.665 E-5	1.70	1.309	.871 E12
.21	.109 E-4	1.52	1.305	.363 E12
.31	.159 E-4	1.36	1.311	.139 E12
.41	.227 E-4	1.23	1.326	.468 E11
.51	.324 E-4	1.09	1.344	.125 E11
.61	.479 E-4	.960	1.360	.238 E10
.71	.755 E-4	.821	1.370	.257 E 9
.81	.135 E-3	.671	1.376	.104 E 8
.91	.336 E-3	.487	1.378	.181 E 6
Radius(km) R				
.10	.208 E 5			
.20	.299 E 5			
.30	.378 E 5			
.40	.453 E 5			
.50	.530 E 5			
.60	.613 E 5			
.70	.701 E 5			
.80	.822 E 5			
.90	.988 E 5			
1.00	.151 E 6			

Table 3

M = 52

X_r	v	T_9	γ	E_v
.01	.364 E-5	1.80	1.334	.950 E12
.03	.491 E-5	1.74	1.323	.858 E12
.11	.962 E-5	1.56	1.306	.452 E12
.21	.156 E-4	1.39	1.307	.175 E12
.31	.229 E-4	1.25	1.318	.603 E11
.41	.327 E-4	1.12	1.332	.175 E11
.51	.472 E-4	.994	1.352	.420 E10
.61	.705 E-4	.870	1.363	.680 E 9
.71	.113 E-3	.745	1.369	.614 E 8
.81	.206 E-3	.607	1.374	.225 E 7
.91	.519 E-3	.438	1.375	.101 E 6

R

.10	.246 E 5
.20	.354 E 5
.30	.448 E 5
.40	.537 E 5
.50	.629 E 5
.60	.728 E 5
.70	.842 E 5
.80	.983 E 5
.90	.119 E 6
1.00	.183 E 6

Table 4

M = 60

X_r	v	T_9	γ	E_v
.01	.555 E-5	1.68	1.324	.627 E12
.03	.728 E-5	1.62	1.314	.556 E12
.11	.133 E-4	1.46	1.302	.281 E12
.21	.208 E-4	1.31	1.307	.106 E12
.31	.297 E-4	1.18	1.321	.386 E11
.41	.415 E-4	1.06	1.339	.786 E10
.51	.587 E-4	.949	1.354	.241 E10
.61	.859 E-4	.835	1.364	.398 E 9
.71	.134 E-3	.718	1.369	.360 E 8
.81	.240 E-3	.567	1.372	.174 E 7
.91	.592 E-3	.430	1.373	.862 E 5

R

.10	.292 E 5
.20	.415 E 5
.30	.519 E 5
.40	.619 E 5
.50	.720 E 5
.60	.828 E 5
.70	.951 E 5
.80	.110 E 6
.90	.126 E 6
1.00	.184 E 6

ding rate of change of the neutrino losses. Tables 2,3, and 4 give conditions at the onset of instability. In each case it took somewhat more than 500 seconds to reach a total kinetic energy of $2 \cdot 10^{48}$ ergs. In the description of each explosion this was chosen, more or less arbitrarily, as the zero point for the time.

5.3. Evolution of 45 Solar Mass Model

At about 63 seconds the kinetic energy reached its peak (during the collapse) of $6.88 \cdot 10^{49}$ ergs. The velocity at the surface was $-1,072$ km/sec. At 73 seconds the nuclear burning reached its peak value of $1.24 \cdot 10^{50}$ ergs/sec. Although the temperature increased slightly after this, oxygen depletion near the center more than offset the temperature increase. The neutrino loss rate was about 200 times smaller, $.635 \cdot 10^{48}$ ergs/sec. At 76 seconds the collapse was halted at the center; the central density and temperature were $1.3 \cdot 10^6$ gm/cc and $3.1 \cdot 10^9$ °K. Table 5 gives conditions throughout the star at this point. At the halt of the collapse about 2.9 solar masses of oxygen were burnt, and about $2.9 \cdot 10^{51}$ ergs liberated. As the star rebounds oxygen depletion and the fall of the temperature quickly cut off the nuclear burning. At 100 seconds the rate had decreased to the neutrino loss rate, about $.2 \cdot 10^{48}$ ergs/sec; a total of 3.3 solar masses of oxygen were burned. Table 6 gives energy generation rates throughout

the evolution.

The effects of convective instability were not significant. At 82 seconds the star became convectively unstable at a mass fraction $X_r = .08$. At 133 seconds the convective zone reached its maximum value of $X_r = .12$. The onset of the convection at a point some distance from the center was a common feature of the three models; it would appear to be due to the following. The high temperature dependence of the neutrino losses creates an increasingly large entropy gradient as the center is approached. Ordinarily nuclear burning is even more sensitive to the temperature; this causes the convection to start at the center. However, in this case the collapse quickly pushed the material to high temperatures where the dependence of the oxygen burning on the temperature is somewhat lower. This and the depletion of oxygen at the center spreads the energy generation over a larger area. The start of convection away from the center is then favored by an initially lower entropy gradient that exists farther out in the star.

Except in the outer few per cent of the mass, no shock wave was observed to develop. This was also true of the other models. (There appeared to be a weak shock near the surface). Ono and Sakashita (1962) investigated an analytical formulation of the progress of a shock wave through a star. Their estimate of the power necessary to generate a shock wave in the interior was

$$3 \text{ E } 46 (M/R)^{2.5} \text{ ergs/sec}$$

where the mass and radius are in terms of those of the sun. This is about $1 \text{ E}53$ ergs/sec, or about 1000 times the actual rate.

After the collapse was halted the basic feature was the increase of the kinetic energy. The 45 solar mass model was the only one in which the total energy remained negative; however, this did not prevent some of the material at the surface from being ejected. It does mean that the entire star would not be disrupted. At 145 seconds the kinetic energy reached a maximum of $1.81 \text{ E}51$ ergs. The surface velocity was 4,337 km/sec. At 189 seconds the surface velocity reached its maximum of 4,652 km/sec. This is only about $1/3$ of the escape velocity at the time of maximum contraction. At 940 seconds about the inner 90% of the star began to collapse again. The central specific volume was $.3 \text{ E}-2$ cc/gm. Slightly more than two periods of the oscillation which was set up were followed. The period was about 1300-1400 seconds. During the first oscillation the central density increased by a factor of 30, and then decreased by a factor of 10. In the second oscillation it increased by a factor of 5, and, during the expansion phase, decreased by a factor of 3. At least initially the oscillations were being rapidly damped out. The chief cause of the damping was probably

the interaction with the ejected material. The evolution was carried out to about 4,000 seconds. Conditions at this point indicated a final velocity at the front of the ejected material of about 3,400 km/sec. From one to two solar masses were ejected. Table 7 gives conditions where the calculation was terminated.

5.4. Evolution of the 52 Solar Mass Model

At 112 seconds the kinetic energy reached its peak during the collapse of $2.64 \text{ E}50$ ergs, with a surface velocity of $-1,849 \text{ km/sec}$. At 118 seconds the oxygen burning reached its maximum value of $3.35 \text{ E}50$ ergs/sec. At 125 seconds the collapse was halted at the center, and the star began to expand. The central density was $1.6 \text{ E}6$ cc/gm, and the central temperature was about $T_0 = 3.3$. Table 8 gives conditions at the time of the halt of the collapse. The neutrino loss rate was $1.98 \text{ E}48$ ergs/sec. This was slightly less than 1% of the nuclear rate. At this time about 6.4 solar masses of oxygen had been burnt. By 139 seconds the oxygen burning rate was reduced to the neutrino loss rate of $.6 \text{ E}48$ ergs/sec. A total of 7.3 solar masses of oxygen were burnt. This made the total energy positive ($2.21 \text{ E} 51$), so a large fraction of the mass of the star should be ejected. Energy generation rates throughout the evolution are given in Table 9.

Table 5

M= 45

X_r	v	T_9	Nuclear Energy Generation (ergs/gm-sec)		Mass Fraction, Oxygen X_{16}
			ϵ_ν	ϵ_n	
.01	.904 E-6	3.01	.536 E14	.599 E16	.1310
.03	.105 E-5	2.92	.447 E14	.128 E17	.3156
.11	.150 E-5	2.66	.243 E14	.505 E16	.9191
.21	.222 E-5	2.42	.136 E14	.251 E16	.9968
.31	.313 E-5	2.19	.710 E13	.114 E14	.9999
.41	.438 E-5	2.01	.389 E13	.415 E12	1.000
.51	.626 E-5	1.81	.176 E13	.102 E11	1.000
.61	.933 E-5	1.61	.663 E12	.121 E 9	1.000
.71	.150 E-4	1.40	.178 E12	.425 E 6	1.000
.81	.276 E-4	1.15	.232 E11	-	1.000
.91	.695 E-4	.844	.388 E 9		1.000
R					
.10	.135 E 5				
.20	.184 E 5				
.30	.227 E 5				
.40	.269 E 5				
.50	.311 E 5				
.60	.358 E 5				
.70	.412 E 5				
.80	.480 E 5				
.90	.580 E 5				
1.00	.899 E 5				

Table 6

M = 45

Time (sec) t	Total Energy (ergs) E_T	Total Kinetic Energy (ergs) E_K	Nuclear Energy Generation (ergs/sec) L_n	Neutrino Losses (ergs/sec) L_ν
0	-.461 E52	.224 E49	.630 E45	.198 E47
45	-.456 E52	.309 E50	.451 E49	.150 E48
59	-.415 E52	.642 E50	.574 E50	.310 E48
66	-.350 E52	.667 E50	.103 E51	.448 E48
76	-.231 E52	.230 E50	.119 E51	.693 E48
85	-.151 E52	.136 E50	.575 E50	.715 E48
100	-.132 E52	.423 E51	.175 E48	.209 E48
112	"	.104 E52	-	-
145	"	.181 E52		
166	"	.169 E52		
197	"	.145 E52		
519	"	.309 E51		
943	"	.171 E51		
1490	"	.381 E51		
1702	"	.161 E51		
1893	"	.240 E51		
2237	"	.120 E51		
2611	"	.141 E51		
3177	"	.977 E50		
3354	"	.134 E51		
3989	"	.975 E51		

Table 7

M = 45

X_r	v	T_9
.01	.470 E-3	.398
.03	.572 E-3	.385
.11	.812 E-3	.346
.21	.119 E-2	.308
.31	.171 E-2	.275
.41	.247 E-2	.250
.51	.372 E-2	.211
.61	.619 E-2	.177
.71	.126 E-1	.137
.81	.695 E-1	.080
.91	.229 E 3	.139 E-1
		velocity(km/sec)
	R	U
.10	.110 E 6	-51
.20	.150 E 6	-83
.30	.185 E 6	-98
.40	.219 E 6	-116
.50	.256 E 6	-135
.60	.298 E 6	-177
.70	.353 E 6	-212
.80	.450 E 6	-334
.90	.182 E 7	278
1.00	.136 E 8	3,506

At 116 seconds convection started at $X_r = .08$. At the time of the reversal of collapse the convective zone spread to $X_r = .28$. The maximum value of the convective luminosity was $4.7 E49$ ergs/sec. The total turbulent energy was $3.3 E49$ ergs, with a maximum speed of the turbulence of 420 km/sec. At 138 seconds the convective zone reached an approximate maximum value of $X_r = .58$. The maximum turbulent energy was $8.6 E49$ ergs; the largest value of the speed of the turbulence was 550 km/sec. This was less than 10% of the speed of sound, and the turbulent energy density less than 1% that of the internal energy. Therefore the dynamic effect of the turbulence was probably quite small. As the entropy gradient in the outer part of the star was small, a slightly larger release of energy would probably have extended the convection to the surface.

At 191 seconds the kinetic energy reached its maximum of $4.88 E51$ ergs. The velocity at the surface was about $6,400$ km/sec. At 310 seconds the surface velocity reached a maximum of $6,774$ km/sec. The evolution was carried out to 1,257 seconds, by which time the surface velocity declined to $6,622$ km/sec. By subtracting the gravitational energy from the kinetic energy at the surface, the final velocity was estimated at $6,500$ km/sec. By finding the point where the velocity equaled the velo-

city of escape, it was found that a minimum of 20 solar masses would be ejected. Since the total energy is positive, it may be that essentially all the mass would be found to be ejected if the evolution were followed long enough. Table 10 gives conditions at the point where the calculation of the evolution was stopped.

5.5. Evolution of the 60 Solar Mass Model

During the collapse the maximum kinetic energy of $.625 E_{51}$ ergs was reached at 137 seconds. The surface velocity was $-2,750$ km/sec. At 142 seconds oxygen burning reached a peak of $.774 E_{51}$ ergs/sec. Neutrino losses were about $\frac{1}{2}\%$ of this. At about 148 seconds the collapse began to be reversed. At this point the nuclear burning rate was $.582 E_{51}$ ergs/sec; the decrease was due to oxygen exhaustion near the center. The central density was $2 E_6$ gm/cc, and the central temperature was about $T_c = 3.6$. Energy release from the α -process never became significant. The collapse was halted before the temperature at the center reached the point where heavier nuclei begin to decompose back into helium. It may be that in a considerably more massive star (e.g., 100 solar masses, if any exist) the collapse would not be reversed until the center reached this point; in that case the collapse might never be stopped. At the reversal of the collapse in the 60 solar mass model about 12.4 solar masses of oxygen had

Table 8 M = 52

X_r	v	T_9	E_ν	E_n	X_{16}
.01	.734 E-6	3.28	.123 E15	.720 E15	.0142
.03	.900 E-6	3.18	.116 E15	.183 E16	.0370
.11	.132 E-5	2.92	.561 E14	.161 E17	.4086
.21	.176 E-5	2.67	.301 E14	.516 E16	.9080
.31	.232 E-5	2.46	.168 E14	.423 E15	.9950
.41	.317 E-5	2.25	.893 E13	.232 E14	.9998
.51	.444 E-5	2.05	.470 E13	.868 E12	1.000
.61	.655 E-5	1.84	.211 E13	.169 E11	1.000
.71	.104 E-4	1.61	.708 E12	.118 E 9	1.000
.81	.190 E-4	1.35	.136 E12	.101 E 6	1.000
.91	.474 E-4	1.00	.471 E10	-	1.000

R Convective Luminosity
(ergs/sec)
 L_c

.10	.136 E 5	.135 E50
.20	.183 E 5	.454 E50
.30	.230 E 5	-
.40	.260 E 5	
.50	.298 E 5	
.60	.340 E 5	
.70	.389 E 5	
.80	.450 E 5	
.90	.541 E 5	
1.00	.837 E 5	

Table 9 M = 52

t	E_T	E_K^*	Total Turbulent Kinetic Energy (ergs) E_C	L_n	L_v
0	-.524 E52	.207 E49		.455 E44	.127 E47
80	-.524 E52	.441 E50		.433 E48	.101 E48
97	-.510 E52	.137 E51		.259 E50	.264 E48
112	-.292 E52	.264 E51		.259 E51	.893 E48
118	-.100 E52	.164 E51	-	.332 E51	.144 E49
125	.719 E51	.401 E49	.328 E50	.222 E51	.198 E49
134	.219 E51	.396 E51	.826 E50	.242 E50	.125 E49
138	.221 E51	.836 E51	.863 E50	.957 E48	.589 E48
143	"	.153 E52	.827 E50	-	-
157	"	.356 E52	.692 E50		
191	"	.487 E52	.503 E50		
315	"	.406 E52	.209 E50		
610	"	.333 E52	.990 E49		
1257	"	.288 E52	.682 E49		

* does not include turbulent energy

Table 10

M = 52

X_r	v	T_9		
.01	.183	.484 E-1		
.03	.249	.469 E-1		
.11	.415	.406 E-1		
.21	.597	.358 E-1		
.31	.833	.320 E-1		
.41	1.25	.276 E-1		
.51	1.85	.241 E-1		
.61	3.01	.202 E-1		
.71	5.53	.164 E-1		
.81	11.7	.126 E-1		
.91	33.9	.851 E-2		
	R	L_c		U
.10	.895 E 6	.153 E46		651
.20	.124 E 7	.257 E45		935
.30	.154 E 7	-		1161
.40	.182 E 7			1390
.50	.213 E 7			1661
.60	.248 E 7			1973
.70	.291 E 7			2368
.80	.351 E 7			2931
.90	.443 E 7			3841
1.00	.719 E 7			6662

been burnt; as in the case of the 52 mass star more than enough energy was released to disrupt the star. Table 11 gives conditions throughout the model at this point.

At 137 seconds convection started at $X_r = .08$. By 148 seconds it had reached $X_r = .56$. The largest value of the convective luminosity was $.21 E_{51}$ ergs/sec. The maximum value of the speed of the turbulence was about 1,000 km/sec. This was about one tenth the speed of sound. As in the previous case this was probably too small for the turbulence to have much dynamic effect. At 156 seconds the front of the convective zone reached $X_r = .82$, and at 162 seconds it reached the surface. These last two figures are not very meaningful. There is no energy generation in the outer half of the star, and the front of the convective zone moved considerably faster than the speed of the turbulence. The convective equations represent a type of diffusion, and so are not very good in describing the motion of the front of the convection zone when it is moving very fast. In the program that was used, the time it takes the convective front to move across a mass zone is the time it takes the mass zone to absorb enough energy to raise its entropy above that of the next zone. In some cases for nearly isentropic material this time may be much less than the time it should take the turbulence to cross it; this makes the front of the convection zone

advance faster than it should. As in the other cases the evolution was too fast by about a factor of 10 for the mixing by convective diffusion to keep the high temperature areas supplied with fuel from the rest of the zone.

As in the previous cases the nuclear energy generation decreased very rapidly after the reversal of the collapse; by 158 seconds it was reduced to the neutrino losses, about $.14 E_{49}$ ergs/sec. A total of 15 solar masses were burned. Table 12 gives the energy generation rates. At 224 seconds the kinetic energy rose to its maximum of $.109 E_{53}$ ergs; the velocity of expansion was 8,741 km/sec. Evolution was carried out to 390 seconds. Table 13 gives conditions at this point. The maximum surface velocity of 8,948 km/sec was reached at 345 seconds. Using the same methods as in the previous case, the final velocity was estimated to be greater than 8,500 km/sec, and at least 40 solar masses were ejected. At the time when the calculations were stopped (390 seconds) convection had carried about $7 E_{49}$ ergs to the surface.

5.6. Summary; Comparison with Observations

Table 14 gives the results for each mass.

Table 11 M = 60

X_r	v	T_0	ϵ_v	ϵ_n	X_{16}
.01	.629 E-6	3.56	.215 E15	.341 E15	.0026
.03	.762 E-6	3.46	.184 E15	.815 E15	.0065
.11	.111 E-5	3.18	.147 E15	.134 E17	.0919
.21	.147 E-5	2.92	.649 E14	.278 E17	.5141
.31	.189 E-5	2.71	.366 E14	.672 E16	.9086
.41	.244 E-5	2.50	.214 E14	.619 E15	.9929
.51	.324 E-5	2.29	.112 E14	.380 E14	.9997
.61	.442 E-5	2.09	.575 E13	.107 E13	1.000
.71	.706 E-5	1.83	.219 E13	.175 E11	1.000
.81	.121 E-4	1.57	.597 E12	.421 E 8	1.000
.91	.278 E-4	1.23	.523 E11	-	1.000
	R	L_c			
.10	.135 E 5	.134 E48			
.20	.182 E 5	.130 E51			
.30	.220 E 5	.209 E51			
.40	.255 E 5	.147 E51			
.50	.290 E 5	.538 E50			
.60	.327 E 5	-			
.70	.368 E 5				
.80	.421 E 5				
.90	.497 E 5				
1.00	.672 E 5				

Table 12

M = 60

t	E _T	E _K *	E _C	L _n	L _v
0	-.563 E52	.221 E49		.322 E43	.932 E46
107	-.565 E52	.918 E50		.571 E48	.152 E48
133	-.314 E52	.576 E51		.428 E51	.124 E49
137	-.105 E52	.625 E51		.617 E51	.196 E49
143	.314 E52	.360 E51	-	.761 E51	.360 E49
148	.668 E52	.541 E49	.311 E51	.582 E51	.476 E49
152	.815 E52	.602 E51	.489 E51	.132 E51	.411 E49
156	.825 E52	.176 E52	.627 E51	.286 E49	.158 E49
159	"	.296 E52	.648 E51	.451 E47	.623 E48
166	"	.533 E52	.623 E51	-	-
174	"	.772 E52	.592 E51		
201	"	.107 E53	.475 E51		
224	"	.109 E53	.389 E51		
390	"	.992 E52	.176 E51		

*does not include turbulent energy

Table 13

M = 60

X_r	v	T_9		
.01	.162 E-1	.125		
.03	.209 E-1	.121		
.11	.279 E-1	.111		
.21	.395 E-1	.975 E-1		
.31	.521 E-1	.881 E-1		
.41	.699 E-1	.791 E-1		
.51	.953 E-1	.706 E-1		
.61	.139	.615 E-1		
.71	.193	.545 E-1		
.81	.333	.441 E-1		
.91	.742	.318 E-1		
	R	L_c		U
.10	.403 E 6	.162 E47		1,519
.20	.544 E 6	.919 E47		2,035
.30	.660 E 6	.777 E47		2,563
.40	.770 E 6	.579 E47		3,000
.50	.881 E 6	.549 E47		3,448
.60	.999 E 6	.497 E47		3,885
.70	.113 E 7	.508 E47		4,522
.80	.129 E 7	.527 E47		5,238
.90	.151 E 7	.398 E47		6,190
1.00	.214 E 7	-		8,943

Table 14

Mass	Solar Masses Ejected	Solar Masses, Oxygen, Burned	Velocity of Expansion(km/sec)
45	1-2	3	3,400
52	> 20	7	6,500
60	> 40	15	8,500

The best known features of Type II supernovae are their light curves; they take perhaps a week to rise to maximum luminosity and then several weeks to decay. The investigation of this was beyond the scope of the evolution followed here. Type II supernovae are observed to expand with a velocity of 5,000-10,000 km/sec. The mass of supernovae remnants is not well known. It is usually estimated to be of the order of several solar masses. One estimate of 60 solar masses was made by Shklovskii (1960). The results of the explosions induced by pair production fit in roughly with these observations.

There is also the question of whether there are enough massive stars to account for these supernovae. It has been estimated that there is one type II supernova per galaxy about every 500 years. The solar luminosity function ϕ (number of stars per cubic parsec per unit visual magnitude on the main sequence in the solar neighborhood) was computed by Sandage (1957) to $M_V = -6$; the mass for this magnitude was estimated to be about 33 solar masses. Here we estimate that ϕ , for more massive objects,

is

$$\phi = .20 \text{ E-8} \times 10^{(M_V + 6)}$$

Assuming the luminosity is proportional to the cube of the mass, and neglecting changes in the bolometric correction, ϕ' , the number of stars per unit solar mass, is

$$\phi' = .6 \text{ E-8} (M/33)^{-7.5}/M$$

The time on the main sequence is estimated to be

$$T = 1.6 \text{ E} 7 (25/M)^2 \text{ years}$$

Taking 33 solar masses as the lower limit for pair production explosions and neglecting any mass loss after the main sequence is left, the number of explosions per cubic parsec is

$$N = \int_{33}^{\infty} dM \phi' / T$$

The values above give $N = 1.5 \text{ E-16/yr}$. When all material is projected onto the central plane of the galaxy, the number of these massive stars per pc^2 is 220ϕ ; the total mass per pc^2 is 55 solar masses (Schmidt, 1959). Taking the mass of the galaxy as 10^{11} solar masses, there will be about one explosion every 15,000 years if the solar neighborhood is representative of the galaxy as a whole. This is too low by about a factor of 30. It might be noted that the relative abundance of these massive stars in young galactic clusters is about 2,500 times as great as in the solar neighborhood. It would be necessary that these clusters be representative of somewhat more than 1% of the

of the mass of the galaxy to provide a sufficient number of massive stars.

Remarks

. It was argued in section 5.1. that if there is any shell burning after neutrino losses become important, it should extend the effective convective zone over much of the envelope (to the point where the envelope becomes so extended that mixing cannot be effectively established during the burning time). Fowler and Hoyle (1964), however, took the mass of the envelope to be $1/3$ of the total mass. If this is correct, the masses given here (which are the effective core masses) should be multiplied by 1.5 to give the total mass.

With the possible exception of the lower mass star, the total amount of oxygen burnt should not be very sensitive to the reaction rate. Most of the oxygen near the center is consumed; a higher rate would just extend the burning region outward somewhat, while a lower rate would still be sufficient to burn most of the oxygen near the center. Since the increase in pressure due to the energy release of the burning is partly responsible for the reversal of the collapse, a lower reaction rate should result in a collapse to a higher temperature. It is estimated that if the rate does not differ from the one used in the calculations by more than a factor of 100, the amount of material consumed should not change by more than a factor of 2.

It now appears that the reduced width, Θ_{α}^2 , for the $C^{12}(\alpha, \gamma)O^{16}$ reaction is .1 (Fowler, 1967). About 25% of the helium is then converted into carbon in these massive stars (Deinzer and Salpeter, 1964). A convective core due to carbon burning should then be formed at a central temperature of about $T_0 = 1.1$. The small amount of neon formed will burn at a higher temperature ($T_0 = 1.3-1.6$). The result will be a somewhat greater central entropy (at the onset of instability) than that found for the models investigated here.

Barkat, Rakavy, and Sack (1967) recently computed the explosion for a star with a core of 40 solar masses. Six solar masses of oxygen were burnt for no convective mixing, and 12 were burnt for instantaneous mixing. The convective mixing for the models investigated here only increased the amount of oxygen consumed by a few per cent. Therefore 6 solar masses should be about the right figure. This is about what would have been burnt for a 50 solar mass version of the models investigated in this paper.

References

- Arnett, D., 1967, submitted for publication
- Barkat, Z., Rakavy, G., Sack, N., 1967, P.R. Let., 18, 379
- Batchelor, G.K., 1953, The Theory of Homogeneous Turbulence,
(Cambridge University Press)
- Chiu, H.Y., 1961, Phys. Rev., 123, 1040
- Colgate, S.A. and White, R.H., 1966, Ap. J., 143, 626
- Cowling, T.G., 1936, Monthly Notices, 96, 42
- Deinzer, W. and Salpeter, E.E., 1964, Ap.J., 140, 499
- Finzi, A. and Wolf, R.A., 1966, submitted for publication
- Fowler, W.A., private communication, 1967
- Fowler, W.A. and Hoyle, F., 1960, Ap. J., 132, 565
- Fowler, W.A. and Hoyle, F., 1964, Ap.J. Supplement 91,
vol. IX, 201
- Ledoux, P., 1958, Handbuch der Physik, vol. LI, 605
- Levine, M.J., 1963, thesis, California Institute of Technology, unpublished
- Ono, Y. and Sakashita, S., 1962, J.Ph.Soc.Jap., 17,
Supplement A-III, 153
- Rakavy, G. and Shaviv, G., 1966, submitted for publication
- Richtmyer, R.D., 1957, Difference Methods for Initial-Value
Problems, (Interscience Publishers, Inc., New York)
- Sandage, A., 1957, Ap.J., 125, 422

Schmidt, M., Ap.J., 129, 243

Schwarzschild, M., 1958, Structure and Evolution of the
Stars, (Princeton University Press)

Shaviv, G., submitted for publication

Shklovskii, I.S., 1960, Soviet Astronomy, 4, 355

Figure 1 outlines the boundary of the area in which γ becomes less than $4/3$ because of electron-positron pair production.

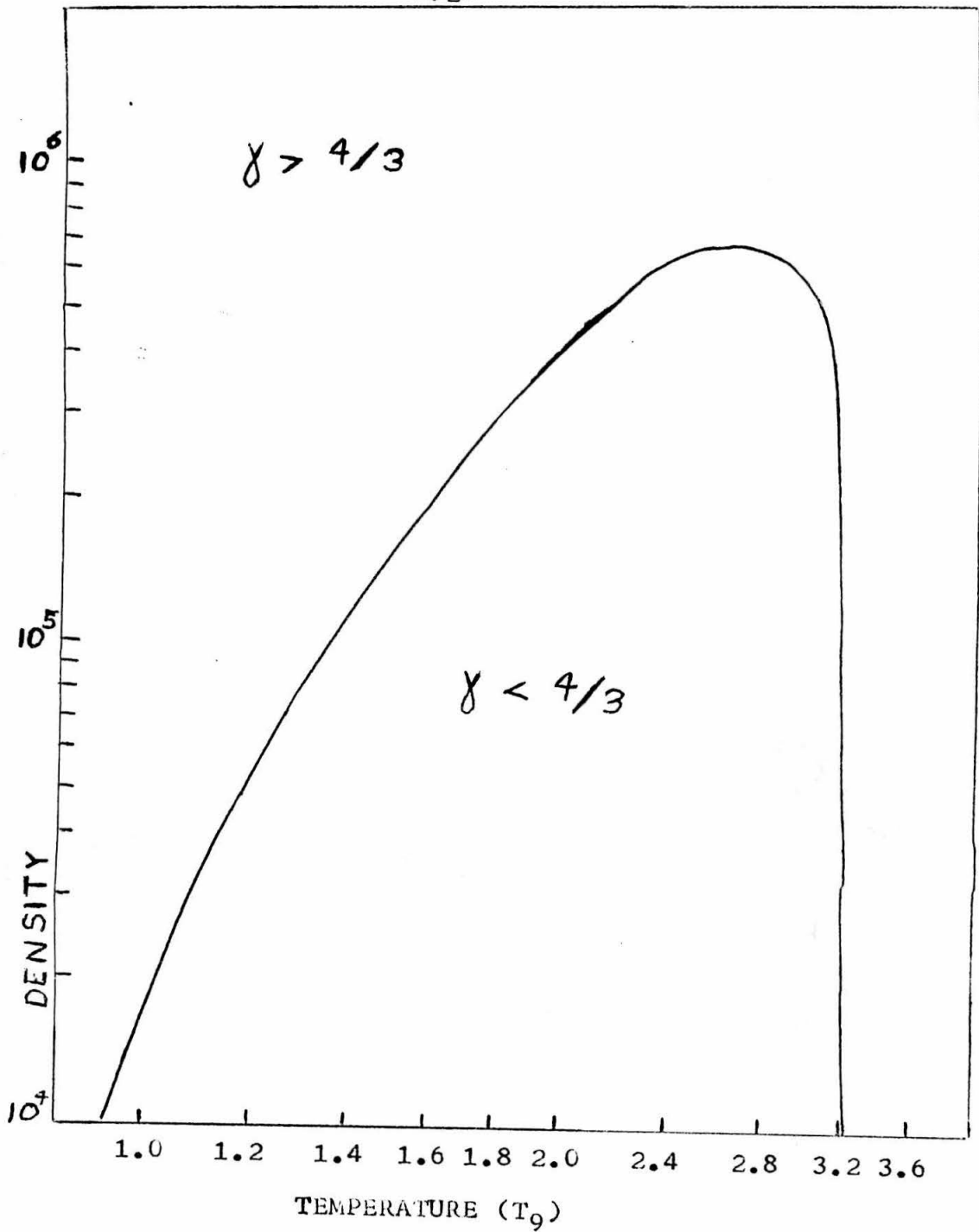


Figure 1